Electronic Supplementary Material (ESI) for Journal of Materials Chemistry A.

Supplementary Material (ESI)

Enhancing the Performance of Indoor Organic Photovoltaics through Precise Modulation of Chlorine Density in Wide Bandgap Random Copolymers

Soyoung Kim, Seon Joong Kim, Gayoung Ham, Ji-Eun Jeong, Donghwa Lee, Eunho Lee, Hyungju Ahn, Hyojung Cha, Jae Won Shim*, and Wonho Lee**

Experimental section

Materials: 2,6-Dibromo-4,8-bis(4-chloro-5-(2-ethylhexyl)thiophen-2-yl)benzo[1,2-b:4,5-b']dithiophene (BDTTCl-Br) and (4,8-bis(4-chloro-5-(2-ethylhexyl)thiophen-2-yl)benzo[1,2-b:4,5-b']dithiophene-2,6-diyl)bis(trimethylstannane) (BDTTCl-Sn) were synthesized according to previous literature.[1] 2,6-Dibromo-4,8-bis(5-(2-ethylhexyl)thiophen-2-yl)benzo[1,2-b:4,5-b']dithiophene (BDTT-Br) was purchased from SunaTech. 2,6-Bis(trimethyltin)-4,8-bis(5-ethylhexyl-2-thienyl)benzo[1,2-b:4,5-b′]-dithiophene (BDTT-Sn) and 1,3-dibromo-5-octyl-4H-thieno[3,4-c]pyrrole-4,6(5H)-dione (TPD-Br) were purchased from Solarmer, Inc. $PC_{71}BM$ was purchased from Brilliant Matter; all monomers were used without further purification.

Synthesis of random copolymers: B30T70 was synthesized following our previous study.[2] The monomers BDTT-Sn (200.0 mg, 0.2962 mmol), BDTT-Br (65.50 mg, 0.08886 mmol), and TPD-Br (87.70 mg, 0.2073 mmol) were polymerized to afford B30T70. Yield: 258.8 mg (93%). Number average molecular weights (M_n) = 20 kg mol^{-1} and dispersity ($Đ$) = 3.7. Elem. Anal. Calcd: C, 69.42; H, 6.90; N, 1.05; O, 2.40; S, 20.03%. Found: C, 69.07; H, 7.01; N, 0.85; O, 2.85; S, 19.49%. A series of random copolymers B30T70-XCl, where X = 2, 4 or 6, was synthesized using different combinations of Cl-free monomers, BDTTCl-Br, and BDTTCl-Sn while fixing TPD-Br (0.7 eq) as shown in **Scheme S1**.

Random copolymer B30T70-2Cl was synthesized using BDTTCl-Br (53.40 mg, 0.06633 mmol), BDTT-Sn (0.2000 mg, 0.2211 mmol), and TPD-Br (0.06550 mg, 0.1548 mmol). Yield: 201 mg (95%); M_n = 41 kg mol^{-1} and $Đ$ = 5.1. Elem. Anal. Calcd: C, 67.92; H, 6.69; N, 1.03; O, 2.34; S, 19.79; Cl, 2.23%. Found: C, 67.35; H, 6.77; N, 0.81; O, 2.73; S, 19.60; Cl, 2.74%

Random copolymer B30T70-4Cl was synthesized using BDTT-Br (45.4 mg, 0.06165 mmol), BDTTCl-Sn (200 mg, 0.2055 mmol), and TPD-Br (60.9 mg, 0.1438 mmol). Yield: 193 mg (93%); M_n = 24 kg mol^{-1}, and $Đ$ = 4.0. Elem. Anal. Calcd: C, 64.66; H, 6.23; N, 0.98; O, 2.23; S, 18.84; Cl, 7.06%. Found: C, 65.73; H, 6.9; N, 0.67; O, 2.45; S, 17.43; Cl, 6.82%

Random copolymer B30T70-6Cl was synthesized using BDTTCl-Br (49.6 mg, 0.06165 mmol), BDTT-Sn (200 mg, 0.2055 mmol) and TPD-Br (60.9 mg, 0.1438 mmol). Yield: 200 mg (95%); M_n = 25 kg mol^{-1}, and $Đ$ = 2.9. Elem. Anal. Calcd: C, 63.36; H, 6.04; N, 0.96; O, 2.19; S, 18.46; Cl, 9.00%. Found: C, 62.73; H, 6.13; N, 0.66; O, 2.58; S, 18.51; Cl, 9.39%

Characterization: The M_n and $Đ$ of polymers were determined by size exclusion chromatography (SEC) using trichlorobenzene as the eluent at a temperature of 140 ℃. To determine the composition of the polymers, EA was conducted using a Thermo Scientific Flash 2000 series instrument. The TGA was performed using a TA Instruments Q500(I) under a nitrogen atmosphere, employing a heating rate of 10 ℃ min^{-1} from 30 ℃ to 500 ℃ to obtain the decomposition temperatures. DSC was measured using DSC200F3 under a nitrogen atmosphere, with a heating and cooling rate of 10 ℃ min^{-1} from 30 ℃ to 300 ℃. The UV-vis absorption spectra and CV were performed following our previous report.[2] For the UV-vis absorption spectra, the samples were analyzed using Shimadzu JP / UV-1900 spectrophotometer. Temperature-dependent absorption measurement in the chlorobenzene solvent state was performed in the range of RT-110 ℃, and the concentration of the solutions was 2.7 μg mL^{-1}. CV was conducted using a WizEIS-1200Premium electrochemical workstation with three electrode configurations. The PESA measurements were conducted using a Riken model AC-2 instrument with a power setting of 5 nW and a power count of 0.5. AFM images were acquired in tapping mode using a Park Systems model XE-100 instrument. The ESP analysis was carried out at B3LYP/6-31* level using spartan'14. 2D-GIWAXS experiments were performed at the 9A U-SAXS beamline of the Pohang Accelerator Laboratory in Korea. The X-rays from the in-vacuum undulator were monochromated (λ= 1.12 Å) with an incidence angle of 0.12°. 2D-GIWAXS patterns were collected by a two-dimensional CCD detector (MX170-HS, Rayonix Inc.). The detector was placed approximately 210 mm from the center of the sample. The incidence angle of the films was set at 0.12˚. To obtain field-effect carrier mobility (μ_{sat}), field effect transistors were fabricated. Pristine and blend films were spin-coated on a 200 nm Si/SiO_2 substrate. A 50 nm thick Au source/drain electrode was deposited using a shadow mask (W: 600 μm & L: 180 μm). The transfer curve was measured to understand the electrical characteristics of the random copolymers. The μ_{sat} was calculated using the following equation. $\mu_{sat} = 2\frac{L}{WC}\left(\frac{\partial\sqrt{I_D}}{\partial V_G}\right)^2$ where, L (μm) is the channel length, W (μm) is the channel width, C (F cm^{-2}) is the specific capacitance of the dielectric layer = 1.62×10^{-8} F cm^{-2}, I_D (μA) is the drain current, V_G (V) is the gate voltage. Finally, the mobility of the fabricated device was calculated by measuring the transfer curves through Keithley 4200. Nanosecond-Second Transient Absorption (ns-s TA) measurements were performed using the pump-probe technique. The TA setup employed for longer timescales uses an Nd:YAG laser (EL-YAG, 6–8 ns pulse width), which generates visible pulses (532 nm), and a third harmonic generator for EL-YAG, which generates UV pulses (355 nm). The probe beam originates from a 150 W Xenon lamp which reflected off the powder sample, and then a monochromator before it impinges onto a PMT-980 photodiode detector. Pump pulses are directed from the laser output to the sample via a liquid light guide and are overlapped with the probe beam at the position of the sample. A comprehensive L900 spectrometer software package acquires data on two different time scales simultaneously: the ns-μs signal is sampled using an oscilloscope (Tektronix MDO3022). Excitation fluences were measured using a pyroelectric energy sensor. *Device fabrication*: All experimental procedures were adapted from existing literature.[2] Photoactive layer solutions were prepared by dissolving a total of 25 mg mL^{-1} in chlorobenzene with 3 vol% 1,8-diiodooctane (DIO), with weight ratio of 1:2 (D:A), and stirred at 45 °C for 3 hour. The photoactive layer was deposited by spin coating at 1000 rpm for 60 s under nitrogen-controlled conditions. To characterize the light performance of organic IPV devices under indoor environment, two different types of artificial light sources were used: an LED lamp (McScience, Suwon, Republic of Korea) with light intensity (I_L: 0.254 mW cm^{-2} at 1000 lx) and an FL (OSRAM DUL-UXSTAR STIC 11 W) with light intensity (I_L: 0.30 mW cm^{-2} at 1000 lx). The active area of the OPV was estimated to be approximately 0.045 cm^2 using an optical microscope.

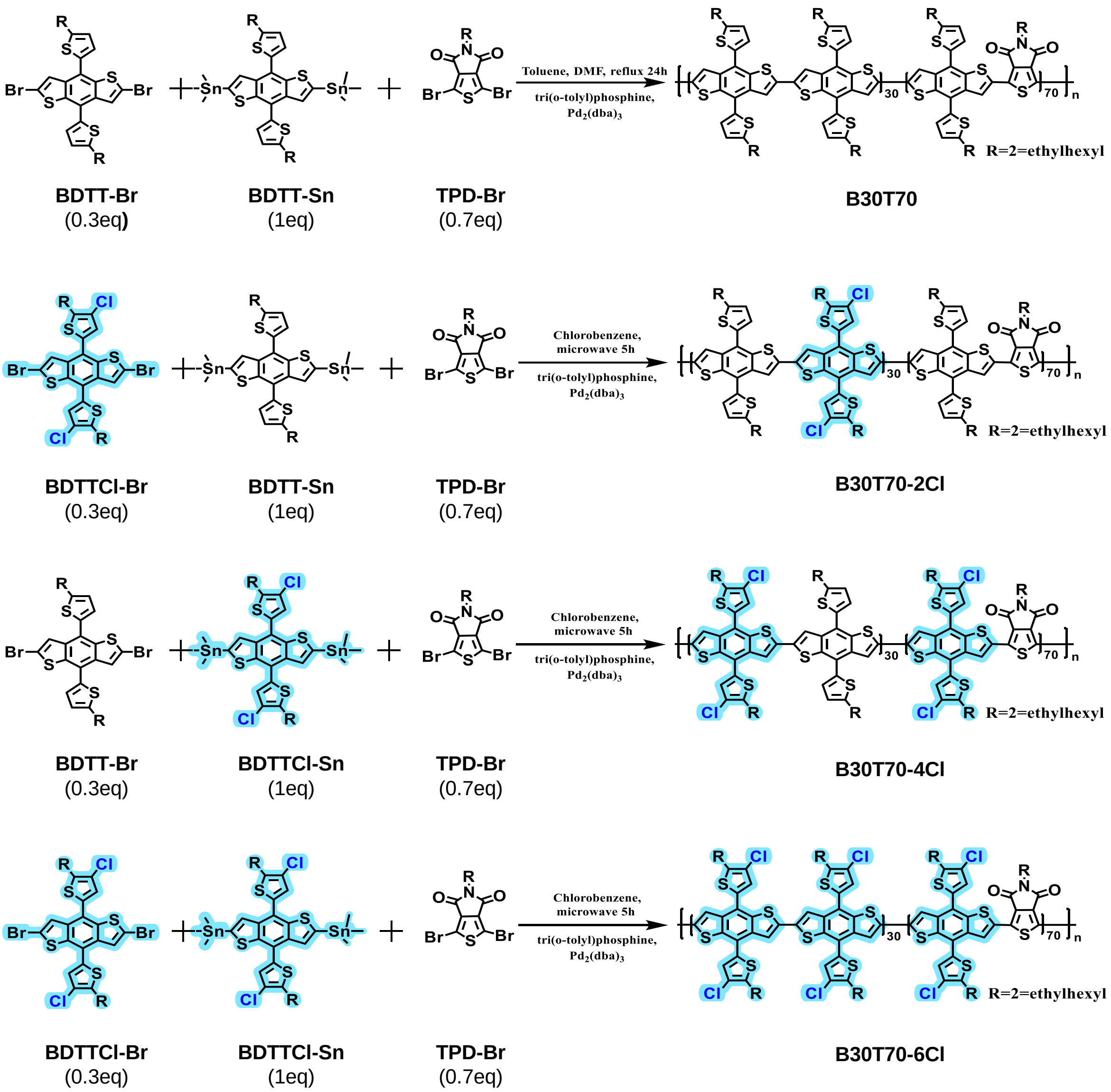

Scheme. S1. Synthetic scheme of B30T70-XCl (X=0, 2, 4, 6).

Table S1. Monomer feed ratio and Cl density of the B30T70-XCl random copolymers.

Polymer	Feed ratio					Cl monomer density
	BDTT-Sn (eq)	BDTT-Br (eq)	BDTTCl-Sn (eq)	BDTTCl-Br (eq)	TPD-Br (eq)	
B30T70	1	0.3	-	-	0.7	0
B30T70-2Cl	1	-	-	0.3	0.7	0.15
B30T70-4Cl	-	0.3	1	-	0.7	0.5
B30T70-6Cl	-	-	1	0.3	0.7	0.65

Table S2. Actual Cl ratio of B30T70-XCl determined by elemental analysis.

Polymer	C (%)	H (%)	N (%)	O (%)	S (%)	Total (%)	Cl (%)
B30T70	69.42[a)]	6.90[a)]	1.05[a)]	2.40[a)]	20.03[a)]	99.8[a)]	0
	69.07[b)]	7.01[b)]	0.85[b)]	2.85[b)]	19.49[b)]	99.27[b)]	0
B30T70-2Cl	67.92[a)]	6.69[a)]	1.03[a)]	2.34[a)]	19.79[a)]	97.77[a)]	2.23[a)]
	67.35[b)]	6.77[b)]	0.81[b)]	2.73[b)]	19.60[b)]	97.26[b)]	2.74[c)]
B30T70-4Cl	64.66[a)]	6.23[a)]	0.98[a)]	2.23[a)]	18.84[a)]	92.94[a)]	7.06[a)]
	65.73[b)]	6.9[b)]	0.67[b)]	2.45[b)]	17.43[b)]	93.18[b)]	6.82[c)]
B30T70-6Cl	63.36[a)]	6.04[a)]	0.96[a)]	2.19[a)]	18.46[a)]	91.01[a)]	9.00[a)]
	62.73[b)]	6.13[b)]	0.66[b)]	2.58[b)]	18.51[b)]	90.61[b)]	9.39[c)]

[a)] Calculated values, [b)] measured values by elemental analysis, and [c)]100-total.

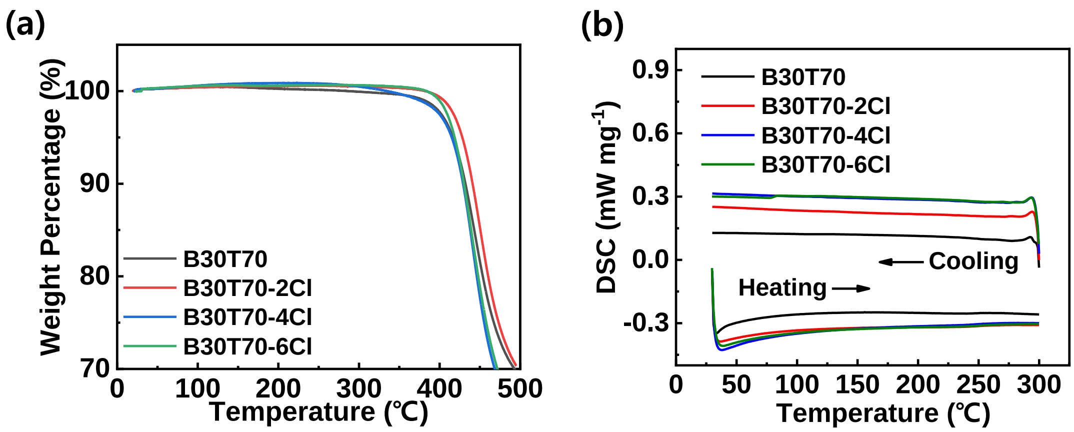

Fig. S1. (a) TGA and (b) DSC thermograms of random copolymers.

Table S3. Optical properties of random copolymers and $PC_{71}BM$ in thin films.

Material	λ_{max} (nm)	λ_{edge} (nm)	E_g^{opt} (eV)
B30T70	554, 601	658	1.88
B30T70-2Cl	555, 601	658	1.88
B30T70-4Cl	553, 598	646	1.92
B30T70-6Cl	554, 596	649	1.91
$PC_{71}BM$	481	721	1.72

Table S4. Maximum efficiencies of photovoltaics under 1-Sun and indoor illumination.

Condition	Polymers	V_{OC} (mV)	J_{SC} (Outdoor: mA cm^{-2}, Indoor: μA cm^{-2})	FF (%)	PCE (%)
AM 1.5G (100 mW cm^{-2})	**B30T70**	916	11.1	73.1	7.4
	B30T70-2Cl	948	11.3	73.1	7.8
	B30T70-4Cl	967	6.8	55.4	3.6
	B30T70-6Cl	996	3.8	63.1	2.4
FL 1000 lx (0.30 mW cm^{-2})	**B30T70**	774	119.5	74.5	22.9
	B30T70-2Cl	806	122.5	76.0	25.0
	B30T70-4Cl	821	74.3	61.3	12.5
	B30T70-6Cl	819	42.1	65.2	7.5
LED 1000 lx (0.254 mW cm^{-2})	**B30T70**	775	95.9	74.4	21.8
	B30T70-2Cl	791	97.8	74.8	22.8
	B30T70-4Cl	810	63.1	61.1	12.3
	B30T70-6Cl	830	32.2	65.9	6.9

Table S5. Comparison of photovoltaic properties under standard AM 1.5G and FL illumination.

Donor:acceptor	**Device type**	**Light source**	**1 Sun PCE (%)**	**Indoor PCE (%)**	**Increase in PCE (fold)**	**ref**
B30T70-2Cl:$PC_{71}BM$		**FL 1000lx**	**7.8**	**25.0**	**3.2**	**Our work**
B30T70:$PC_{71}BM$		**FL 1000lx**	**7.4**	**22.9**	**3.1**	
P3HT:$PC_{71}BM$	Fullerene based	FL 300lx	2.4	5.8	2.4	3
PCDTBT:$PC_{71}BM$		FL 300lx	6.0	16.6	2.8	
PTB7:$PC_{71}BM$		FL 300lx	6.8	14.6	2.1	
P3HT:ICBA		FL 500lx	4.97	14.36	2.9	4
P3HT:$PC_{60}BM$		FL 500lx	3.75	9.74	2.6	
PBDTTT-EFT:$PC_{70}BM$		FL 500lx	7.22	13.4	1.9	
PDTBTBz-2Fanti:$PC_{71}BM$		FL 1000lx	7.0	18.6	2.7	5
PBDB-T:$PC_{71}BM$		FL 1000lx	6.2	12.5	2.0	
P3HT:$PC_{71}BM$		FL 1000lx	2.7	7.7	2.9	
PTB7:$PC_{71}BM$		FL 1000lx	6.2	10.5	1.7	
PBDB-TSCl:IT-4F	Non-fullerene based	FL 1000lx	13.4	20.1	1.5	6
CD1:ITIC		FL 1000lx	8.5	17.9	2.1	7
CD1:PBN-10		FL 1000lx	7.9	26.2	3.3	
CD1:PBN-14		FL 1000lx	7.9	22.9	2.9	8
PCDTBT:PDTSTPD:$PC_{71}BM$	Multi-component based	FL 300lx	6.0	20.8	3.5	9
PBDB-T:PTB7Th:ITIC-Th:$PC_{70}BM$		FL 1000lx	7.9	14.7	1.9	10

Table S6. SC values of fullerene and non-fullerene acceptors.

Type	Acceptor	SC_A	ref
Fullerene acceptors	$PC_{61}BM$	17.4	11
	$PC_{71}BM$	17.4	
Fused acceptors	IT-4F	64.1	12
	ITIC-4Cl	51.9	11
	ITIC	54.5	
	COi8DFIC	86.1	12
	Y6	71.0	
	BTP-eC9 (Y7)	80.0	
	L8-BO	71.1	
	CH1007	69.8	
	M34	67.5	
	4TIC-4F	59.8	
	IFIC-i-4F	91.2	
	IEICO-4F	72.6	
	F8IC	80.7	
	FOIC	74.1	
	O-IDTBR	56.0	11
Non-fused acceptors	CO1-4F	64.8	12
	W1	50.0	
	Ph04T-3	49.1	
	4T-3	28.4	
	NoCA-5	76.1	
	TPDC-4F	64.8	
	BN-2F	53.2	
	DBT-HD	35.4	
	C60T-4F	58.8	
	A4T-16	33.3	
	2BTh-2F	38.4	
	o-4TBC-2F	45.9	
	PTB4Cl	33.5	

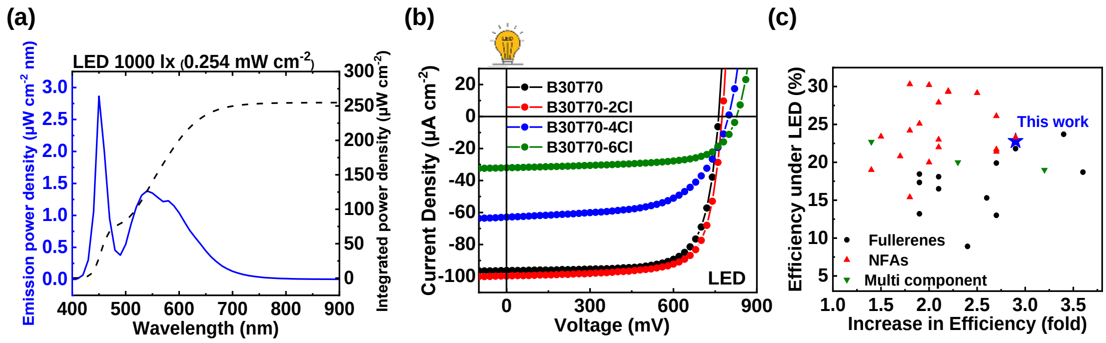

Fig. S2. (a) Emission power and integrated emission power spectra of LED (b) *J*-*V* curve under illumination of LED 1000 lx. (c) Comparison of PCE and increase in the PCE of IOPVs under LED illumination.

Table S7. Photovoltaic parameters under illumination of LED 1000 lx.

Polymer	Condition	V_{OC} (mV)	J_{SC} (μA cm^{-2})	FF (%)	PCE_{avg}[a] (P_{max}) (%)
B30T70	LED 1000 lx (Irradiance 0.254 mW cm^{-2})	774 ± 10	95.7 ± 1.7	73.6 ± 0.7	21.1 ± 0.5 (21.8)
B30T70-2Cl		783 ± 8	97.7 ± 0.6	74.1 ± 0.9	22.0 ± 0.9 (22.8)
B30T70-4Cl		802 ± 7	63.4 ± 0.8	60.3± 1.1	12.0 ± 0.2 (12.3)
B30T70-6Cl		819 ± 9	31.2 ± 1.0	65.4 ± 1.0	6.7 ± 0.3 (6.9)

[a] Average PCE values obtained from 5 different devices

Table S8. Comparison of photovoltaic properties under standard AM 1.5G illumination and LED.

Donor:acceptor	Device type	Light source	1 Sun PCE (%)	Indoor PCE (%)	Increase in PCE (fold)	ref
B30T70-2Cl:PC$_{71}$BM	Fullerene based	**LED 1000 lx**	**7.8**	**22.8**	**2.9**	**Our work**
B30T70:PC$_{71}$BM		**LED 1000 lx**	**7.4**	**21.8**	**2.9**	
PCDTBT:PC$_{71}$BM		LED 300 lx	5.3	18.7	3.5	13
P3HT:ICBA		LED 500 lx	4.97	13.47	2.7	4
P3HT:PC$_{60}$BM		LED 500 lx	3.75	9.04	2.4	
PBDTTT-EFT:PC$_{70}$BM		LED 500 lx	7.22	13.37	1.9	
WF3F:PC$_{71}$BM		LED 500 lx	9.44	17.34	1.8	14
PTQ10:PC$_{61}$BM		LED 500 lx	7.5	19.9	2.7	15
PTB7-Th:PC$_{71}$BM		LED 1000 lx	9.67	18.55	1.9	16
PBDB-TF:PC$_{71}$BM		LED 1000 lx	8.43	18.1	2.1	17
PBDB-T:PC$_{71}$BM		LED 1000 lx	6.2	15.7	2.5	5
PDTBTBz-2Fanti:PC$_{71}$BM		LED 1000 lx	7.0	23.7	3.4	
PPDT2FBT:PC$_{71}$BM		LED 1000 lx	7.7	16.5	2.1	18
PTB7-Th:PC$_{70}$BM		LED 890 lx	8.43	11.63	1.4	19
PBDB-TF:ITCC	Non-fullerene based	LED 1000 lx	10.3	22	2.1	17
PBDB-TF:IT-4F		LED 1000 lx	12.2	20.8	1.7	
PBDB-TF:IO-4Cl		LED 1000 lx	9.7	26.1	2.7	20
PM6:Y6-O		LED 1200 lx	16.5	30.31	1.8	21
PB2:FTCC-Br		LED 1000 lx	14.8	30.2	2	22
S2:LBT-DCl		LED 1000 lx	13.2	25.1	1.9	23
S2:LBT-DF		LED 1000 lx	13.4	24.2	1.8	
PM6:FCC-Cl		LED 1000 lx	13.0	27.9	2.1	24
D18:FCC-Cl		LED 1000 lx	13.1	29.4	2.2	
D18:FCC-Cl-4Ph		LED 1000 lx	13.12	29.3	2.2	25
CD1:ITIC		LED 1000 lx	8.7	15.4	1.8	7
CD1:PBN-10		LED 1000 lx	8.0	21.7	2.7	
CD1:PBN-14		LED 1000 lx	7.9	21.4	2.7	8
PBDB-T:BTA3		LED 1000 lx	8.0	23.3	2.9	26
PTQ10:IDIC		LED 1200 lx	9.9	20	2.0	27
PTQ10:IDIC-Br		LED 1200 lx	10.8	23	2.1	

PBDB-TF:HDO-4Cl		LED 1000 lx	15.6	23.4	1.5	28
PBDB-TF:GS-ISO		LED 1000 lx	11.6	29.15	2.5	29
PM6:M36		LED 1000 lx	13.8	19	1.4	30
PM6:Y6:Y–Th2		LED 1000 lx	16.0	22.7	1.4	31
PCDTBT:PDTSTPD:$PC_{71}BM$	Multi-component based	LED 300 lx	6	19	3.2	9
J52-F:PM7:BTA3		LED 300 lx	8.8	20	2.3	32

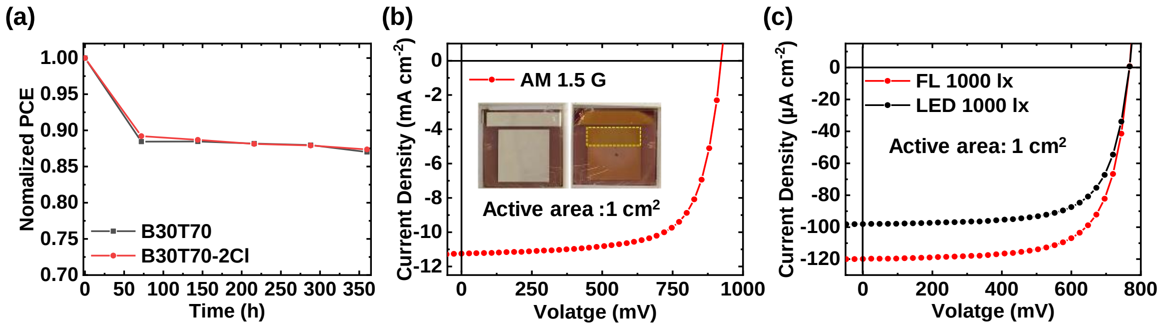

Fig. S3. (a) Stability test under continuous LED illumination (2000 lx). *J-V* curves for large-area devices based on B30T70-2Cl under (b) 1-Sun and (c) indoor lighting conditions.

Table S9. Large-area efficiency of B30T70-XCl:$PC_{71}BM$ based device under 1-Sun, FL, and LED illumination.

Condition	Polymer	V_{OC} (mV)	J_{SC} (Outdoor: mA cm^{-2}, Indoor: μA cm^{-2})	FF (%)	PCE[a)] (%)
AM 1.5G (100 mW cm^{-2})	**B30T70**	898 ± 4	11.1 ± 0.1	69.5 ± 1.2	6.9 ± 0.1
	B30T70-2Cl	922 ± 10	11.2 ± 0.2	70.2 ± 0.9	7.2 ± 0.2
	B30T70-4Cl	953 ± 8	6.4 ± 0.1	47.2 ± 1.5	2.9 ± 0.2
	B30T70-6Cl	978 ± 7	3.5 ± 0.3	58.4 ± 0.7	2.0 ± 0.1
FL 1000lx (0.30 mW cm^{-2})	**B30T70**	741 ± 5	118.4 ± 2.1	70.1 ± 1.9	20.4 ± 0.5
	B30T70-2Cl	767 ± 7	120.0 ± 1.4	70.5 ± 2.3	21.5 ± 0.4
	B30T70-4Cl	793 ± 13	75.3 ± 1.7	57.9 ± 1.8	11.5 ± 0.5
	B30T70-6Cl	801 ± 8	42.7 ± 0.8	61.6 ± 1.2	7.0 ± 0.3
LED 1000lx (0.254 mW cm^{-2})	**B30T70**	736 ± 9	96.2 ± 1.5	70.3 ± 1.5	19.6 ± 0.4
	B30T70-2Cl	770 ± 6	98.2 ± 1.1	71.0 ± 2.1	21.1 ± 0.5
	B30T70-4Cl	789 ± 11	61.2 ± 1.6	58.2 ± 1.6	11.0 ± 0.3
	B30T70-6Cl	803 ± 7	32.4 ± 1.3	61.7 ± 0.8	6.3 ± 0.2

a) Avereage PCE values obtained from 5 different devices

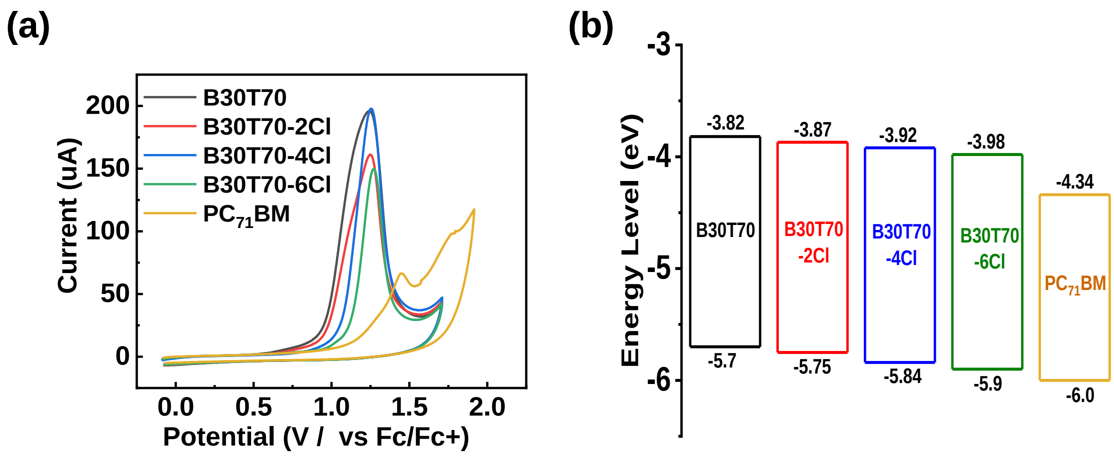

Fig. S4. (a) CV of the random copolymers and $PC_{71}BM$, along with (b) the corresponding energy level diagram.

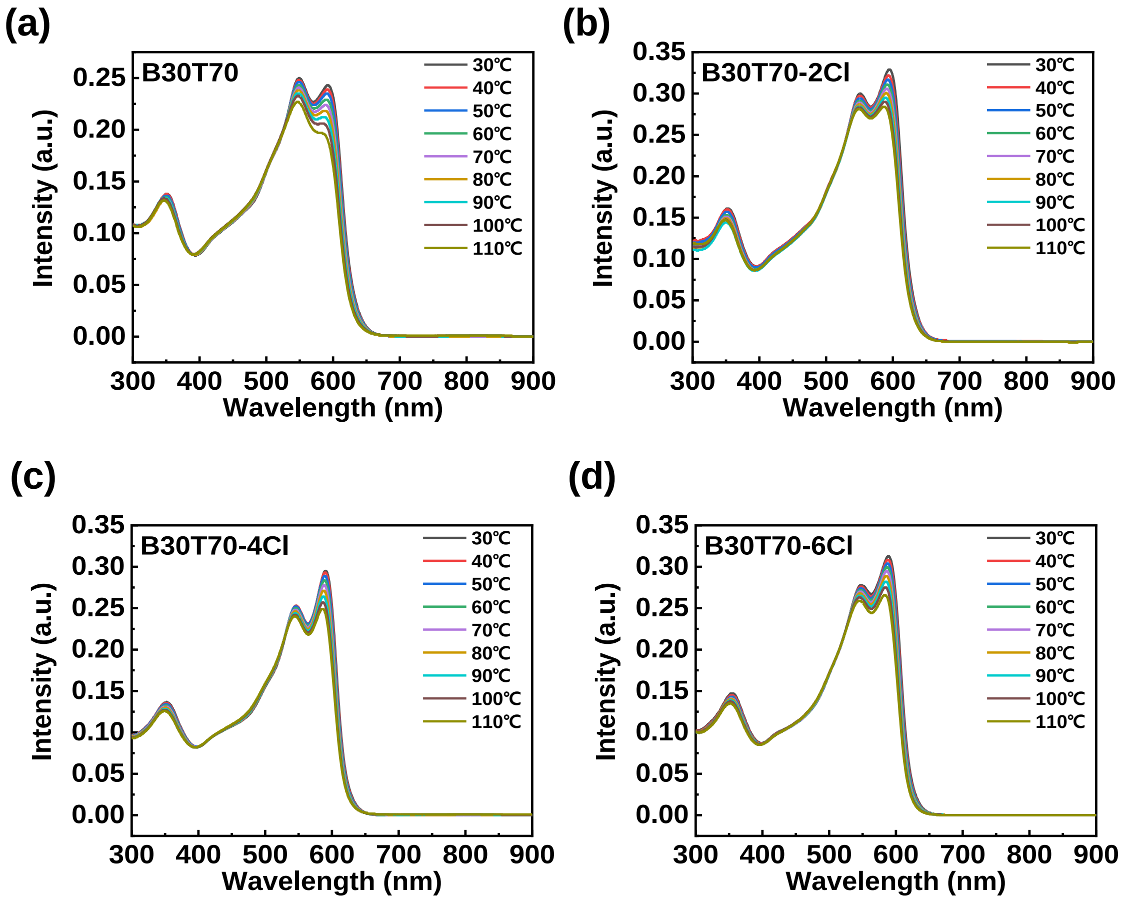

Fig. S5. Temperature-dependent UV-vis absorption spectra of random copolymers.

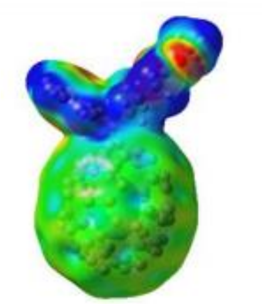

Fig. S6. ESP of $PC_{71}BM$[33]

Table S10. Exciton dissociation probability of B30T70-XCl:$PC_{71}BM$ based devices.

Material	AM 1.5G			Indoor		
	J_{SC}	J_{sat}	P_{diss} (J_{SC}/J_{sat})	J_{SC}	J_{sat}	P_{diss} (J_{SC}/J_{sat})
B30T70	10.9	11.07	0.98	117.2	119.73	0.98
B30T70-2Cl	11.0	11.70	0.94	120.7	121.67	0.99
B30T70-4Cl	6.7	N.A	N.A	75.1	N.A	N.A
B30T70-6Cl	3.6	N.A	N.A	41.2	N.A	N.A

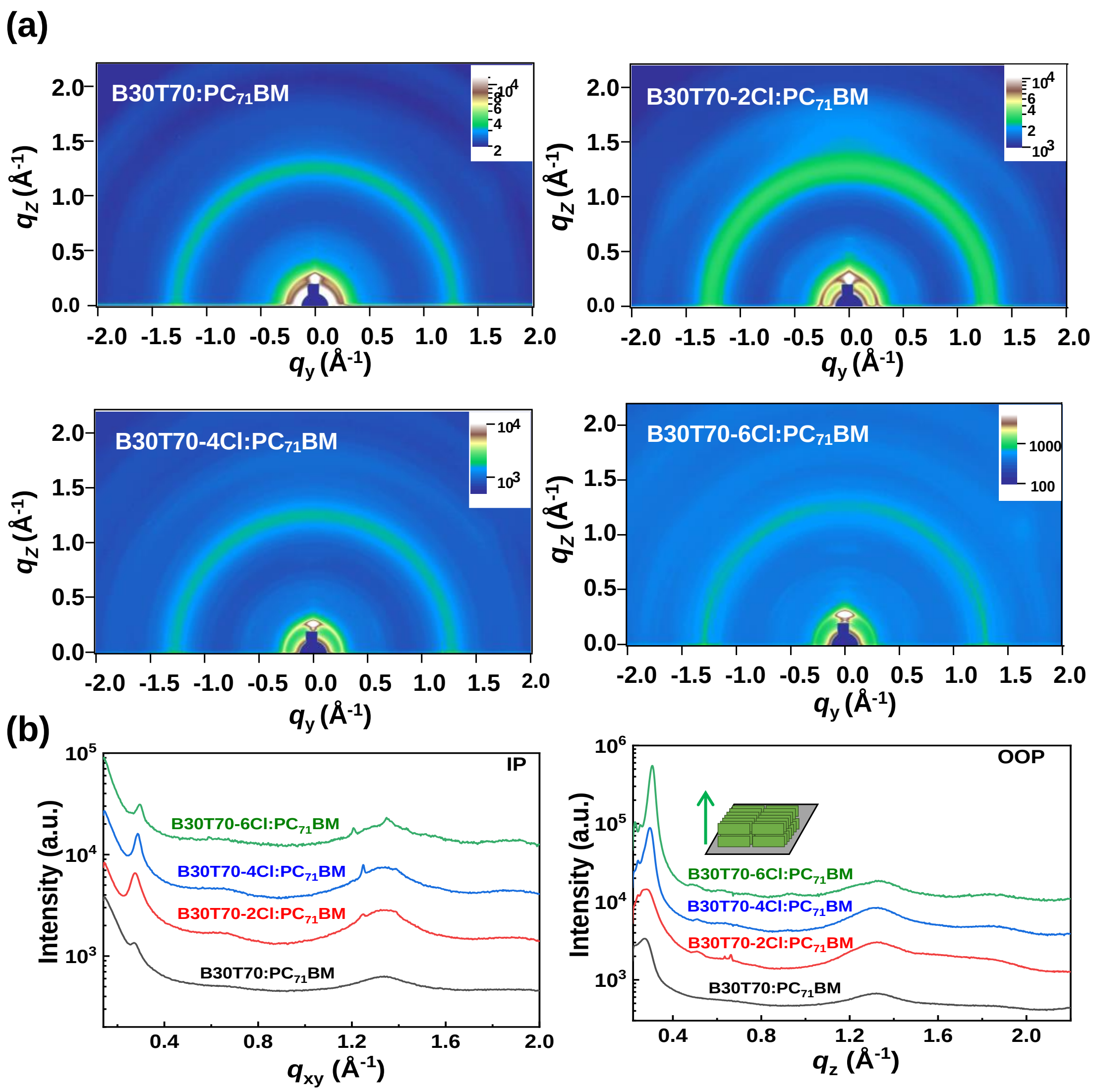

Fig. S7. (a) 2D-GIWAXS patterns and (b) diffraction profiles of in-plane and out-of plane line-cut profiles of blend films.

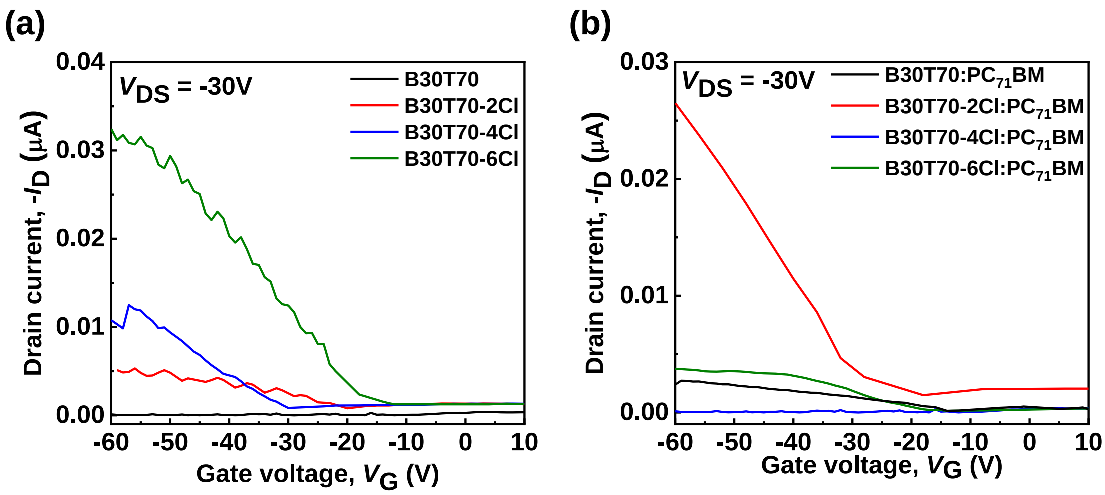

Fig. S8. Transfer curves of OFETs for (a) B30T0-XCl and (b) B30T0-XCl:$PC_{71}BM$ blends.

Table S11. Charge mobility values obtained from OFETs.

	B30T70 ($cm^2\ V^{-1}\ s^{-1}$)	B30T70-2Cl ($cm^2\ V^{-1}\ s^{-1}$)	B30T70-4Cl ($cm^2\ V^{-1}\ s^{-1}$)	B30T70-6Cl ($cm^2\ V^{-1}\ s^{-1}$)
Pristine	N/A	1.67×10^{-5}	2.64×10^{-4}	5.04×10^{-4}
Blend	5.26×10^{-5}	6.73×10^{-4}	N/A	1.17×10^{-4}

References

1 S. Zhang, Y. Qin, J. Zhu and J. Hou, *Adv. Mater.*, 2018, **30**, 1800868.

2 J. Kim, M. A. Saeed, S. H. Kim, D. Lee, Y. Jang, J. S. Park, D. Lee, C. Lee, B. J. Kim, H. Y. Woo, J. W. Shim and W. Lee, *Macromol. Rapid Commun.*, 2022, **43**, 2200279.

3 H. K. H. Lee, Z. Li, J. R. Durrant and W. C. Tsoi, *Appl. Phy. Lett.*, 2016, **108**, 253301.

4 S. Yang, Z. Hsieh, M. L. Keshtov, G. D. Sharma and F. Chen, *Sol. RRL*, 2017, **1**, 1700174.

5 Y. You, C. E. Song, Q. V. Hoang, Y. Kang, J. S. Goo, D. Ko, J. Lee, W. S. Shin and J. W. Shim, *Adv. Funct. Mater.*, 2019, **29**, 1901171.

6 S. Park, H. Ahn, J. Kim, J. B. Park, J. Kim, S. H. Im and H. J. Son, *ACS Energy Lett.*, 2019, **5**, 170-179.

7 Z. Ding, R. Zhao, Y. Yu and J. Liu, *J. Mater. Chem. A*, 2019, **7**, 26533-26539.

8 J. Wang, Y. Gao, Y. Yu, R. Zhao, L. Zhang and J. Liu, *Org. Electron.*, 2021, **92**, 106134.

9 H. Yin, J. K. W. Ho, S. H. Cheung, R. J. Yan, K. L. Chiu, X. Hao and S. K. So, *J. Mater. Chem. A*, 2018, **6**, 8579-8585.

10 M. Nam, H. Y. Noh, J. Kang, J. Cho, B. K. Min, J. W. Shim and D. Ko, *Nano Energy*, 2019, **58**, 652-659.

11 R. Po, G. Bianchi, C. Carbonera and A. Pellegrino, *Macromolecules*, 2015, **48**, 453-461.

12 D. Luo, C. J. Brabec and A. K. K. Kyaw, *Nano Energy*, 2023, **114**, 108661.

13 H. Yin, S. Chen, S. H. Cheung, H. W. Li, Y. Xie, S. W. Tsang, X. Zhu and S. K. So, *J. Chem. C*, 2018, **6**, 9111-9118.

14 R. Singh, C. L. Chochos, V. G. Gregoriou, A. D. Nega, M. Kim, M. Kumar, S. Shin, S. H. Kim, J. W. Shim and J. Lee, *ACS Appl. Mater. Interfaces*, 2019, **11**, 36905.

15 X. Rodríguez-Martínez, S. Riera-Galindo, J. Cong, T. Österberg, M. Campoy-Quiles and O. Inganäs, *J. Mater. Chem. A*, 2022, **1**, 1768-1779.

16 M. Nam, S. Baek and D. Ko, *Appl. Surf. Sci.*, 2020, **526**, 146632.

17 Y. Cui, H. Yao, T. Zhang, L. Hong, B. Gao, K. Xian, J. Qin and J. Hou, *Adv. Mater.*, 2019, **31**, 1904512.

18 S. Shin, C. W. Koh, P. Vincent, J. S. Goo, J. Bae, J. Lee, C. Shin, H. Kim, H. Y. Woo and J. W. Shim, *Nano Energy*, 2019, **58**, 466-475.

19 S. Mori, T. Gotanda, Y. Nakano, M. Saito, K. Todori and M. Hosoya, *Jpn. J. Appl. Phy.*, 2015, **54**, 71602.

20 Y. Cui, Y. Wang, J. Bergqvist, H. Yao, Y. Xu, B. Gao, C. Yang, S. Zhang, O. Inganäs, F. Gao and J. Hou, *Nat. Energy*, 2019, **4**, 768-775.

21 L. Ma, Y. Chen, P. C. Y. Chow, G. Zhang, J. Huang, C. Ma, J. Zhang, H. Yin, A. M. Hong Cheung, K. S. Wong, S. K. So and H. Yan, *Joule*, 2020, **4**, 1486-1500.

22 T. Zhang, C. An, Y. Xu, P. Bi, Z. Chen, J. Wang, N. Yang, Y. Yang, B. Xu, H. Yao, X. Hao, S. Zhang and J. Hou, *Adv. Mater.*, 2022, **34**, 2207009.

23 X. Li, S. Luo, H. Sun, H. H. Sung, H. Yu, T. Liu, Y. Xiao, F. Bai, M. Pan, X. Lu, I. D. Williams, X. Guo, Y. Li and H. Yan, *Energy Environ. Sci.*, 2021, **14**, 4555-4563.

24 F. Bai, J. Zhang, A. Zeng, H. Zhao, K. Duan, H. Yu, K. Cheng, G. Chai, Y. Chen, J. Liang, W. Ma and H. Yan, *Joule*, 2021, **5**, 1231-1245.

25 S. Luo, F. Bai, J. Zhang, H. Zhao, I. Angunawela, X. Zou, X. Li, Z. Luo, K. Feng, H. Yu, K. S. Wong, H. Ade, W. Ma and H. Yan, *Nano Energy,* 2022, **98**, 107281.

26 Z. Chen, T. Wang, Z. Wen, P. Lu, W. Qin, H. Yin and X. Hao, *ACS Energy Lett.,* 2021, **6**, 3203.

27 C. L. Radford, P. D. Mudiyanselage, A. L. Stevens and T. L. Kelly, *ACS Energy Lett.*, 2022, **7**, 1635-1641.

28 Y. Xu, H. Yao, L. Ma, Z. Wu, Y. Cui, L. Hong, Y. Zu, J. Wang, H. Y. Woo and J. Hou, *Mater. Chem. Front.,* 2021, **5**, 893-9.

29 P. Bi, S. Zhang, J. Ren, Z. Chen, Z. Zheng, Y. Cui, J. Wang, S. Wang, T. Zhang, J. Li, Y. Xu, J. Qin, C. An, W. Ma, X. Hao and J. Hou, *Adv. Mater.,* 2021, **34**, 2108090.

30 X. Zhou, H. Wu, B. Lin, H. B. Naveed, J. Xin, Z. Bi, K. Zhou, Y. Ma, Z. Tang, C. Zhao, Q. Zheng, Z. Ma and W. Ma, *ACS Appl. Mater. Interfaces,* 2021, **13**, 44604.

31 Y. Cho, T. Kumari, S. Jeong, S. M. Lee, M. Jeong, B. Lee, J. Oh, Y. Zhang, B. Huang, L. Chen and C. Yang, *Nano Energy,* 2020, **75**, 104896.

32 Y. Bai, R. Yu, Y. Bai, E. Zhou, T. Hayat, A. Alsaedi and Z. Tan, *GEE,* 2021, **6**, 920-928.

33 H. Yao, Y. Cui, D. Qian, C. S. Ponseca, A. Honarfar, Y. Xu, J. Xin, Z. Chen, L. Hong, B. Gao, R. Yu, Y. Zu, W. Ma, P. Chabera, T. Pullerits, A. Yartsev, F. Gao and J. Hou, *J. Am. Chem. Soc.,* 2019, **141**, 7743.